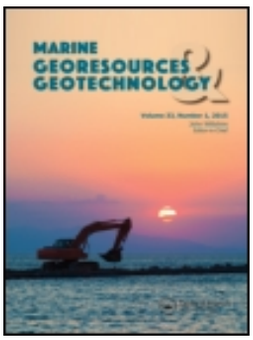

Marine Georesources & Geotechnology

ISSN: 1064-119X (Print) 1521-0618 (Online) Journal homepage: http://www.tandfonline.com/loi/umgt20

Artificial neural network modelling of cross-shore profile on sand beaches: The coast of the province of Valencia (Spain)

Isabel López, L. Aragonés, Y. Villacampa & P. Compañ

To cite this article: Isabel López, L. Aragonés, Y. Villacampa & P. Compañ (2017): Artificial neural network modelling of cross-shore profile on sand beaches: The coast of the province of Valencia (Spain), Marine Georesources & Geotechnology, DOI: 10.1080/1064119X.2017.1385666

To link to this article: http://dx.doi.org/10.1080/1064119X.2017.1385666

Artificial neural network modelling of cross-shore profile on sand beaches: The coast of the province of Valencia (Spain)

Isabel López*

Department of Civil Engineering, University of Alicante, San Vicente del Raspeig, Spain

L. Aragonés

Department of Civil Engineering, University of Alicante, San Vicente del Raspeig, Spain

Y. Villacampa

Department Applied Mathematics, University of Alicante, San Vicente del Raspeig, Spain

P. Compañ

Department of Computer Science and Artificial Intelligence, University of Alicante, San Vicente del Raspeig, Spain

*Address correspondence to Isabel López, Department of Civil Engineering, University of Alicante, San Vicente del Raspeig 03690, Spain. E-mail: isalopu.il@gmail.com

ABSTRACT

The paper describes the training, validation, testing and application of models of artificial neural networks (ANN) for computing the cross-shore beach profile of the sand beaches of the province of Valencia (Spain). Sixty ANN models were generated by modifying both the input variables as the number of neurons in the hidden layer. The input variables consist of wave data

and sedimentological data. To select and evaluate the performance of the optimal model, the following parameters were used: R^2, absolute error, mean absolute percentage error and percentage relative error. Finally, the results are compared with the numerical model proposed by Aragonés et al. (2016b) for the equilibrium profile in the study area. The results show a mean absolute error of 0.21 m compared to 0.33 m Aragones' model, significantly improving the results of the numerical model in the bar area around de Valencia Port. In addition, when comparing the results with other methods currently used (Dean's or Vellinga formulation), the errors of these compared to ANN are of the order of 167% and 1538% higher, respectively.

KEYWORDS: artificial neural network, beach nourishment, beach profile, d_{50}, models, sand beach

1. Introduction

An important problem found along coastlines around the world is the erosion of the beaches (Allen 1981). To combat the erosion, actions are carried out on the coast, such as dikes, breakwaters and/or beach nourishments (Crain, Bolten, and Bjorndal 1995; Hamm et al. 2002), for which it is important to characterize properly morphodynamics of the operating area and the morphology of the cross-shore beach profile (Larson and Kraus 1995; Muñoz-Pérez and Medina 2001; Muñoz-Perez and Medina 2010).

The morphology of a beach is mainly controlled by wave climate, tide and sediment characteristics (Boon and Green 1988; Bernabeu, Medina, and Vidal 2003). The prediction of beach profile evolution under the action of waves and currents is one of the most important tasks in coastal engineering because of its influence on coastal erosion (Grasso et al. 2009). Even though cross-shore sediment fluxes are usually a few orders of magnitude smaller than longshore

transport, the cross-shore beach profile has a strong influence on longshore velocity profiles and therefore on longshore sediment fluxes (Muñoz-Perez et al. 1999; Plant, Ruessink, and Wijnberg 2001). The beach profile is the result of the trade-off between onshore and offshore fluxes. The direction of the cross-shore fluxes is a key point for predictive tools and is closely related to the nonlinear characteristics of the incoming waves such as asymmetry and velocity skewness (Bailard 1981; da Silva, Temperville, and Seabra Santos 2006).

The characterization of the morphology of the cross-shore profiles has evolved over the years from simple mathematical equations defining the equilibrium beach profile (Bruun 1954; Dean 1977; Vellinga 1983; Vellinga 1984), to models (mathematical, numerical, probabilistic, reverse, etc.) for predicting beach profile changes (Stive and de Vriend 1995; Masselink and Li 2001). Process-based mathematical and numerical models are one of the main approaches for the prediction of cross-shore beach profile changes. Deterministic process-based models can either be relatively simple or can incorporate sophisticated hydrodynamic models to calculate the hydrodynamics and morphological response over relatively large areas (Neill, Elliott, and Hashemi 2008). Using numerical modelling, several models can be developed and linked to study cross-shore beach profile. For that, a wave model, tidal current model, sediment transport model and finally a morphological model should be developed, validated using field data and linked to each other for a specific study site (Ranasinghe et al. 2004; Neill, Elliott, and Hashemi 2008). However, such techniques require considerable computational effort. In addition, there are still compelling discrepancies between model results and measured data (Iglesias et al. 2009), which may be due to uncertainties in understanding nearshore processes such as wave breaking, wave reflection, refraction, diffraction and sediment transport (Jones, Petersen, and Kofoed-Hansen 2007) and also can derive by inaccuracy in surveying . Accordingly, other methods such as Artificial Intelligence

(AI) have been introduced in this area, which are less expensive compared with physical-based numerical models (Hashemi, Ghadampour, and Neill 2010).

AI, in common with other data-based approaches, makes use of only the measured data, and is a practical tool which can be used to predict changes to the coastline as a response to changes in wave, currents and tidal climates (Muñoz-Pérez and Medina 2001; Bernabeu, Medina, and Vidal 2003; Muñoz-Perez and Medina 2010). This tool is particularly useful in coastal application because many coastal engineers are interested in prediction rather than deep understanding of the process (Hashemi, Ghadampour, and Neill 2010). In recent years, AI techniques such as artificial neural networks (ANNs) have been previously successfully applied to coastal engineering problems. Such as: plant geometry bay beaches (Iglesias et al. 2009), wind–wave analysis (Browne et al. 2007; Herman, Kaiser, and Niemeyer 2009), wave prediction (Kalra et al. 2005; Lee 2008), coastal water level (Huang et al. 2003; Ghorbani et al. 2010), location and behavior of the bars (Pape et al. 2007; Yan, Zhang, and Wai 2008) or seasonal changes in beach profiles (Hashemi, Ghadampour, and Neill 2010).

The purpose of this study is to investigate the potential of ANN to predict the cross-shore beach profile of sand beaches in a case study (Coast of the province of Valencia, Spain). To this end, first, the variables that may influence the formation of the profile were studied. Some of the considered variables are related to the maritime climate (wave height $H_{s,12}$, period and probability of occurrence (frequency) of the most energetic, most frequent and perpendicular waves) and to the sediment properties (median sediment size (D_{50}), real sample density, material density and porosity). Finally, some ANN were generated (different input variables and number of hidden layers) and the architecture that best represents the cross-shore beach profiles in the study area was selected.

2. Study Area

The study area is located on the east of Spain, covering the 96.7 km of coast of the province of Valencia (39º28'30.7" 00º22'33"W). Among the 45 beaches along the coast, only the 28 beaches not influenced by breakwaters or capes are studied (**Figure 1**). They are long sandy beaches near of delta fans, alluvial cones, dunes, lagoons, capes or ports.

The seabed are composed, mainly, by fine and coarse sand. In the north of the port of Valencia, a large area covered with marine vegetation can be found. In the south, there are some rocky areas mainly near cliffs. However, the profiles used are outside the influence of these elements (**Figure 1a–c**).

The tides in the study area are small. The maximum values reach 75 cm when astronomical tides (30 cm) are affected by meteorological factors (Ecolevante 2006).

3. Material and Methods

In the developed methodology, first the variables that may be related to the formation of the profile (maritime climate and sedimentology) are analysed. While in the second part, the process for the generation of neural networks and the selection of the optimal architecture is described.

3.1. Bathymetric profiles

To obtain the cross-shore profiles, the bathymetry of the "Estudio ecocartográfico de las provincias de Valencia y Alicante (Ecolevante 2006)" conducted by the Directorate General of Coasts was used. This bathymetry was obtained using two multibeam and a single-beam probe from the coastline to a depth of –40 m, with a vertical accuracy of ±15 cm (Ecolevante 2006).

By using a GIS, 140 beach profiles were obtained (at least two profiles per beach, see **Table 1**). These profiles were divided into fifteen points (x, y), of which y_i will be the outputs of the ANNs. The 15 points were chosen so that the x_i was constant for all profiles, and reach, at least, the depth of closure (DoC), calculated according Birkemeier (1985). The x_i values considered are: x_1 = 10 m, x_2 = 20 m, x_3 = 40 m, x_4 = 60 m, x_5 = 80 m, x_6 = 100 m, x_7 = 125 m, x_8 = 150 m, x_9 = 175 m, x_{10} = 200 m, x_{11} = 250 m, x_{12} = 300 m, x_{13} = 350 m, x_{14} = 400 m and x_{15} = 450 m. The points are closer to the beginning of the profile and further apart from the 100 m from the coast, to represent adequately the concave shape of the profiles (Aragonés et al. 2016a).

The profiles of a single season are valid (at least in this area) to characterize the profile of the beach, as Aragonés et al. (2016a) indicates when comparing these profiles with the mean profile obtained from precision profiles (± 2 cm) Taken over 20 years in both summer and winter season, the error committed is less than 8%. Therefore, profiles of a single season can be used without making big mistakes.

3.2. Maritime climate

Wave data were obtained from directional buoys of Valencia 2630 (39°30'57.6''N 0°12'17.9''E, 260 m deep), which belongs to the network "REDEXT" of Public Agency Puertos del Estado (2016). For the study, different wave heights (H), periods (T), directions (Dir), and frequencies (f, probability of occurrence) were taken into account.

Throughout the paper will be denoted the wave height as H, the peak period as T and the probability of occurrence of each direction as f. On the other hand, among the different directions that affect the beach, it will distinguish between: i) the normal direction of the wave (that affects perpendicular to the beach) and which will be denoted as PC. Ii) The direction with the highest

probability of occurrence (most of the waves incident on the beach come from that direction) and which will be denoted as MF. And iii) direction that presents the highest wave heights, the highest wave height incident to the beach (peak energy wave), peak period and associated direction will be determined and will be denoted as ME.

All the data were obtained using the program AMEVA v1.4.3 (IHCantabria 2013)., and all wave heights are referred to the wave height that is exceeded 12 hours a year ($H_{s,12}$).

Moreover, the wave height at break (H_b) was obtained by two methods: i) using the methodology proposed by the Recommendation for Marine Works (ROM 0.3-91 1991), which considers refraction and shoaling, and ii) using the formulation proposed by Komar and Gaughan (1972) according to equation 1.

$$H_{b,K\&G} = H_o \cdot 0.56 \left(H_o / L_o \right)^{-1/5} \qquad (1)$$

Where H_o is the wave height that is exceeded 12 hours a year in deep water and L_o is the wavelength in deep water obtained from equation 2, in which T is the period associated with H_o.

$$L_o = \frac{g \cdot T^2}{2\pi} \qquad (2)$$

Given that the objective is to obtain the mean real profile of the beach, long-term wave data (in this case 2006-2016) will be used. Otherwise, if we used data from a single season what it would be got would be the real profile of that season. For example, if a large storm occurs during a season and uses that wave height data for the ANN, the profile obtained will be the one formed on the beach due to the storm, which will be very different from the average real profile of the beach.

3.3. Sedimentological samples

Sedimentological samples were obtained from a survey conducted by the University of Alicante in 2013 and from a report published by Dirección General de Costas (Ecolevante 2006). For the 28 studied beaches, 393 samples of the dry beach (14 or 15 sample per beach) and 540 of the wet beach (19 or 20 samples per beach) up to the bathymetric –12 m were analysed.

The sample extraction was done using the following procedure: using a Van Veen's grab the sample is extracted and saved in a bucket to be labelled. After being packed into bags the samples were transported in an icebox to the laboratory. The median sediment size (D_{50}), real sample density (ρ_m), the material density (ρ_s) and the porosity (p) for each of the dry beach samples, and the median sediment size (D_{50}) of the sample obtained at the DoC (Birkemeier 1985) were obtained following the UNE 103 101 1995, the UNE 7050-2 1997 and the UNE 103 100 1995. Also the following scientific literature was taken into account: Román-Sierra, Muñoz-perez, and Navarro-Pons (2013); Syvitski (2007).For the characterization of the cross-shore profiles, the data obtained from the nearest sample to each profile were used.

3.4. Artificial neural networks modelling

The artificial neural network, as the name implies, employs the model structure of a neural network which is very powerful computational technique for modelling complex non-linear relationships particularly in situations where the explicit form of the relation between the variables involved is unknown (Gallant 1993). The basic structure of an ANN model is usually comprised of three distinctive layers, the input layer, where the data are introduced to the model and computation of the weighted sum of the input is performed, the hidden layer or layers, where data are processed, and the output layer, where the results of ANN are produced. Each layer consists of

one or more basic element(s) called a neuron or a node. A neuron is a non-linear algebraic function, parameterized with boundary values (Karunanithi et al. 1994). The signal passing through the neuron is modified by weights and transfer functions. This process is repeated until the output layer is reached (Govindaraju 2000). The number of neurons in the input, hidden and output layers depends on the problem. If the number of hidden neurons is small, the network may not have sufficient degrees of freedom to learn the process correctly. On the other hand, if the number is too high, the training will take a longer time and the network may over-fit the data (Karunanithi et al. 1994).

In this study, three-layer feed-forward neural networks (A single hidden layer was used) with back propagation (BP) learning were constructed for computation of the cross-shore profile of sand beaches. A feed-forward neural network (FFNN) is very powerful in function optimization modelling and has extensively been used for the prediction of different elements related to coastal engineering (Browne et al. 2007; Herman, Kaiser, and Niemeyer 2009; Iglesias et al. 2009; Pape et al. 2007).

3.4.1. Back propagation neural network and learning algorithm

The back propagation (BP) is a commonly used learning algorithm in ANN application. It uses the back propagation (BP) of the error gradient. This training algorithm is a technique that helps distribute the error in order to arrive at a best fit or minimum error. After the information has gone through the network in a forward direction and the network has predicted an output, the back propagation algorithm redistributes the error associated with this output back through the model, and weights are adjusted accordingly. Minimization of the error is achieved through several iterations. One complete cycle is known as the "epoch". Each neuron in a layer is connected to

every neuron in the next layer. These links are given a synaptic weight that represents its connection strength (Govindaraju 2000). Although, traditional BP uses a gradient descent algorithm to determine the weights in the network, it computes rather slowly due to linear convergence.

To improve speed, the Levenberg-Marquardt Algorithm (LMA), which is much faster as it adopts the method of approximate second derivative (Wang 2004) was used here. The LMA is similar to the quasi-Newton method in which a simplified form of the Hessian matrix (second derivative) is used. The Hessian matrix can be approximated as equation 3 and 4 (Hagan and Menhaj 1994; Kişi and Uncuoglu 2005).

$$H = J^T \cdot J \quad (3)$$

$$g = J^T \cdot e \quad (4)$$

in which J is the Jacobian matrix which contains first derivatives of the network errors with respect to the weights and biases, and e is a vector of network errors. One iteration of this algorithm can be written as equation 5:

$$\chi_{k+1} = \chi_k - \left[J^T \cdot J + \mu I \right]^{-1} \cdot J^T \cdot e \quad (5)$$

where μ is the learning rate, I is the identity matrix and χ represents connection weights (Dedecker et al. 2004). During training, the learning rate μ is incremented or decremented by a scale at weight updates. When μ is zero, this is just Newton's method, using the approximate Hessian matrix. When μ is large, this becomes gradient descent with a small step size (Karul et al. 2000).

Bayesian regularization (BR) is a training algorithm that updates the weights and bias values according to LMA optimization (Mackay 1992; Foresee and Hagan 1997). It minimizes a combination of squared errors and weights, and then determines the correct combination so as to produce a network that generalizes well (Pan, Lee, and Zhang 2013). BR introduces network weights into the training objective function, which is denoted as $F(\omega)$ in equation 6 and further explained by Yue, Songzheng, and Tianshi (2011).

$$F(\omega) = \alpha E_{\omega} + \beta E_D \quad (6)$$

Where E_{ω} is the sum of the squared network weights and E_D is the sum of network errors. Both α and β are the objective function parameters. In the BR framework, the weights of the network are viewed as random variables, and then the distribution of the network weights and training set are considered as Gaussian distribution.

The α and β factors are defined using the Bayes' theorem. The Bayes' theorem relates two variables (or events), A and B, based on their prior (or marginal) probabilities and posterior (or conditional) probabilities (Li and Shi 2012). After finding the optimum values for α and β for a given weight space, the algorithm moves into LMA phase where Hessian matrix calculations take place and updates the weight space in order to minimize the objective function. Then, if the convergence is not met, algorithm estimates new values for α and β and the whole procedure repeats itself until convergence is reached Yue, Songzheng, and Tianshi (2011).

MATLAB (MathWorks, Inc., Natwick, MA) was used for analyzing the BR Artificial Neural Network (BR) and LM Artificial Neural Network (LMA). To prevent overtraining, develop predictive ability, and eliminate superiors' effects caused by the initial values, the algorithms of

BR and LMA were trained independently 50 times for each generated model. In order to achieve the minimum error in the less computing time, in this study, the training process is stopped if: 1) it reaches the maximum number of iterations; 2) the performance has an acceptable level; 3) the estimation error is below the target; or 4) the LMA μ parameter becomes larger than 10^{10}.

3.4.2. Input data

To determine which parameters would be used as inputs to the neural network, correlations between each of the studied variables and each of the profile points (outputs) were analysed using the statistical software SPSS.

From the results it follows that $H_{o,PC}$, $H_{b,K\&G}$ and $D_{50,\ dry\ beach}$ are the variables that best define the cross-shore profile. However, it can be observed that at the end points of the profile, the frequency perpendicular to the coast – f (PC) – has a certain influence. Furthermore, $H_{b,K\&G}$, as already explained, is obtained from H_o (PC) and T (PC), so it was decided to generate several neural networks with different input variables, to obtain the one that best simulates the cross-shore beach profile. The generated networks are:

1) ANN 1: D_{50}, H_o and f
2) ANN 2: D_{50}, H_b and f
3) ANN 3: D_{50}, H_o,T and f

To determine the size of the sample for training there is no recommendation or rule. However, training values usually range from 70-80% of the total sample. In our case, tests were performed with values of 70, 75 and 80%, obtaining very similar results. That is why and because our sample has a relatively small size, it was decided to choose an intermediate size of 75%. In addition, since for the network adjustment the program selects the training and test groups in a

random manner, that is, with the same starting data, different models can be obtained (ANN). That is why each ANN (with the same starting data) was run 50 times, to verify that the results were always similar and did not depend on the chosen groups of training or test.

Therefore, for ANN identification, the set of wave and sedimentology data (independent variables) for each model (140 profiles × 3 or 4 variables) was divided into three sub-sets. The calibration (or training), validation and test data subsets comprised of 105 (75%), 14 (10%) and 21 (15%) samples each, respectively. Thus, for the model input (independent variables), the training, validation and test data sets have dimensions of 105 profiles × 3 or 4 variables, 14 profiles × 3 or 4 variables, and 21 profiles × 3 or 4 variables, respectively. The output variables correspond to the 15 points defining the profile $(y_1, y_2, \ldots y_{15})$.

In view of the requirements of the neural computation algorithm, the raw data of both the independent and dependent variables were normalized to an interval by transformation. The transformation modifies the distribution of the input variables so that it matches the distribution of the estimated outputs. Here, all the variables are transformed to the same ground-uniform distributions on −1, + 1. The ANNs were applied to provide a non-linear relationship between sets of inputs comprised of some selected characteristic variables and the network outputs (points of the cross-shore beach profile).

3.4.3. Optimization of the ANN structure and modelling performance criteria

In optimization of the networks, the number of neurons used in the hidden layer ranged from 1 to 20, training networks using Bayesian Regularization and Levenberg-Marquardt algorithms, obtaining better results with the first method.

The optimal architecture of the ANN models and its parameter variation were determined based on the Pearson coefficient (R^2) of the training, validation and test sets. Since the data sets for training, validation and test are randomly selected, 50 executions were carried out for each model. So the criterion for selecting the optimal model was to obtain the highest value of R^2 with the smallest dispersion of results in the 50 executions.

To determine the performance of the selected network model, three different criteria were used: absolute error (equation 7), Mean Absolute Percentage Error (MAPE) (equation 8) and percentage relative error (equation 9).

$$e = |r_i - o_i| \quad (7)$$

$$MAPE = \frac{1}{n}\sum_{i=1}^{n}\left|\frac{r_i - o_i}{r_i}\right| \quad (8)$$

$$\delta = \sqrt{\frac{\sum_{i=1}^{n}(r_i - o_i)^2}{(n-p)\frac{1}{n}\sum_{i=1}^{n}(r_i)^2}} \quad (9)$$

Where r_i corresponds to the measured values, o_i with the values obtained from the network, n is the number of values and p is the number of free parameters of expression.

Finally, the results were compared with the numerical model developed by Aragonés et al. (2016b) to obtain the equilibrium profile in the study area. The results were also compared with the formulations of Dean (1977) and Vellinga (1983, 1984) (supplementary material), obtaining errors much larger than the model of Aragonés and the ANN. This model approximates the profile by potential equation (equation 10), where the parameter A depends on the median sediment size

in the dry beach (D_{50}), the porosity, the wave steepness (H_o/L_o) and its associated frequency, to the wave height $H_{s,12}$ perpendicular to the coast.

$$y = A \cdot x^{2/3} \qquad (10)$$

4. Results

First, the results of the study of the correlations between the different analysed variables and each of the points of the profile that are part of the output of the neural network are shown (**Table 2**). As can be seen, the correlation values are generally low, with H_o (PC), $H_{b,K\&G}$, Dir (PC) and $D_{50,\ dry\ beach}$ the variables that have greater relationship with all points, with an average in absolute value of 0.222, 0.216, 0.190 and 0.134, respectively. Also, the variable f (PC) highlights, although it has an absolute mean value of 0.105, at looking at the endpoints (x > 300 m), the values are higher than 0.16 in all cases.

Figure 2 shows the R^2 value obtained for each ANN model. As can be seen, the results are very similar for all models, where the ANN 1 (H_o, f and D_{50}) presents the best results with a high value of R^2 (0.9745 ± 0.0005) and low dispersion during 50 executions. ANN 2 (H_b, f and D_{50}) also shows good results (0.9747 ± 0.0021). Among these networks, the ANN 1 [3–3–15] is chosen because it has fewer neurons in the hidden layer and/or a smaller number of inputs.

Figure 3 shows the absolute error on the selected network and the model of Aragonés et al. (2016b) for each profile. The mean error for the ANN is 0.21 m, with a maximum value of 0.57 m in the profile 16P, and a minimum value of 0.04 m in the profile 132P. While in the Aragonés' model, the mean error is 0.33 m, reaching a maximum of 0.78 m in the 46P profile. In **Figure 4**, this same error for each of the studied beaches is displayed. In this case, the maximum error is 0.33 m for the ANN and 0.62 m for the Aragonés' model, producing on the beach 6.

Finally, the MAPE (Equation 8) and the percentage relative error (Equation 9) were calculated. When analysing these errors in each of the beaches (**Figure 5**) it shows that the MAPE of the ANN is less than 15% at all beaches, except for the beaches 7, 18 and 28, where errors are 26 %, 18% and 51%, respectively. As for the percentage relative error of the ANN, it is less than 10%, except for the first 7 beaches. Among these 7 beaches, beach 4 stands out as having a value of 60%. However, the values of these two errors for the Aragonés' model are 38% and 78% higher, respectively.

5. Discussion

Most of the world's coasts are in regression. To calculate the volume of sand required for nourishment, coastal engineers often use different formulations proposed to obtain the equilibrium profile. However, most beaches that are in regression do not count for their nourishment with a previous profile on balance that suits your features and local factors, hence after nourishment can present a statement of erosion or accretion higher than expected. In addition, as a result of using formulas or equations that do not include the characteristics of the study area, large volume errors are often committed. Therefore, in this paper is intended to generate a neural network model that allows obtaining the cross-shore profile of sand beaches more accurately that other methods as the different equilibrium profile formula.

First, an analysis of linear correlations between each of the profile points and the different studied variables was performed (**Table 2**). This analysis shows that the factors most correlated with the cross-shore profile are those related to the waves perpendicular to the coast, concretely, the wave height in deep water and the breaking wave height obtained according to Komar and Gaughan (1972) (0.222 and 0.216, respectively). When observing the correlations between

variables and each of the studied points of the profile, it is observed that the frequency of the waves perpendicular to the coast has a good relationship with the endpoints of the profile (x > 300 m), although the correlation with the total profile is not too good (0.105). Also other dimensionless parameters as the steepness (H / L), Dean's (H / wT) show very low correlations below 0.120. Regarding sedimentology, most formulations concerning beach profile are related to the median sediment size (D_{50}) (Vellinga 1984; Dean 1991; Kriebel, Kraus, and Larson 1991). In this study, different sedimentological parameters were analysed, and found that among all the D_{50} in the dry beach is the one that has greater relationship with the cross-shore profile (0.134).

For all this, and given that correlations represent linear relationships between two variables, which does not mean that they do not directly affect the profile of the beach when the variables act together. Therefore, it was decided to generate 60 neural networks using different input variables in order determining the individual influence of each one of the variables, and choose the model that gives better results. The inclusion of the variable T (PC) in the last neural network is intended to check how this variable affects, individually, the model, since to obtain $H_{b,K\&G}$ is used both T (PC) and H_o (PC).

Among the different generated ANN, architecture [3-3-15] for the ANN 1 was chosen for being the most stable architecture (less dispersion during 50 executions) with the highest mean value of the coefficient of Pearson (**Figure 2**). This shows that although correlations indicate a good linear relationship between the outputs and inputs (*e.g.* H_b), when combined together by a nonlinear such as neural networks, model their influence on the profile is not as significant as might be expected in first moment. The greater dispersion of the ANN 2 can be due to the inaccuracy of the values of the wave height at break, since they have been obtained by theoretical formulations and not by direct measurement.

On the other hand, for evaluating the performance of the model, various statistical parameters were studied (Equation 7, 8 and 9). By analysing these parameters, it was observed that the neural network improves the results compared to numerical model obtained by Aragonés et al. (2016b) for the equilibrium profile in the study area. Thus, it is observed that the mean absolute error of the ANN is 36.3% lower than the numerical model (0.21 m vs. 0.33 m). The MAPE and the percentage relative error also exhibit an improvement over the numerical model; these errors were 27.5% and 43.9% lower. The results were also compared with other methods such as the Dean's (1977) and Vellinga's (1983, 1984) formulation, and it was observed that the mean error of these methods was 167% and 1538% greater than the ANN error (supplementary material). By analysing in detail the errors, it could be seen that the greatest errors occur mainly on the beaches located near the port of Valencia (Beaches 4, 5, 6 and 7). These beaches present the singularity of being in a zone of active bars between 100–200 m from the coast; these bars affect 13 of the studied profiles, representing less than 10% of the profiles tested throughout the study area, so the network is not able to learn effectively their singularities (**Figure 6**). If the same methodology were applied only to beaches with fixed or active bars, it is likely that the model improved considerably. Although, a study of variables should be performed again, since possibly the influence of the different variables in the profile would vary, and it would even have to study other possible variables that could affect the formation and movement of the bars, as for example the maximum wave height, period, etc. Nevertheless, the results obtained by the ANN in this area are lower (41.5% absolute error, 34% MAPE and 48.9% percentage relative error) than those committed by the model proposed by Aragonés et al. (2016b). All this would result in a lower volume error when calculating the amount of sand needed in beach nourishment, and therefore a lower economic cost. This reduction in the required volume of sand is estimated to be around 3000 m^3/beach, which

would save about 24000 – 45000 € (assuming a cost of 8 – 15 €/m^3). This cost savings certainly compensate the largest computational cost of the ANN versus the simplicity of the numerical model.

Furthermore, the ANN developed here is based on the definition of the cross-shore beach profile in fifteen points separate so that its characteristics are defined generally. However, given the good results provided by the network when simulating the profile with just fifteen points, if greater precision in the profile definition would be needed, it could increase the number of points that define the profile, although this would require more computing time.

6. Conclusions

For modelling the cross-shore profile of sand beaches, different artificial neural networks were considered, with different input variables and different number of neurons in the hidden layer. The used input variables were selected primarily from the study of correlations, from which it was obtained that the variables that had a greater relationship with the beach profile were the wave height perpendicular to the coast in deep waters and in the break point. The criterion for selection of the best model was getting the highest R^2 with the smallest dispersion of results in the 50 executions carried out for each model. Thus, it was found that the network [3–3–15] offered the best results, where the input variables were formed by H_o, f and D_{50}, concerning the waves perpendicular to the coast.

The results were compared with the numerical model presented by Aragonés et al. (2016b) for the equilibrium profile in the study area. It was observed that the mean absolute error committed by the ANN was 0.21 m while for the model of Aragonés et al. (2016b) amounted to 0.33 m. In addition, the network offered better results in the bar area located near the port of

Valencia. However, to improve the results obtained in the area a larger number of profiles affected by bars would be needed, since the number of profiles affected by these elements represents only 9.3% of the total. Increasing the number of profiles with bars would allow the ANN to determine the relationships between the input variables and the points of the profile more precisely, thus providing better results in those profiles.

Therefore, these models can be used to predict the cross-shore beach profile. In addition, if necessary could increase the number of points that define the profile to improve the accuracy of the profile, although this would increase the computation time.

Acknowledgements

The authors want to thanks the Jefatura Provincial de Costas de Alicante and Organismo Público Puertos del Estado for the information provided has enabled this study.

This research has been partially funded by Universidad de Alicante through the project "Estudio sobre el perfil de equilibrio y la profundidad de cierre en playas de arena" (GRE15-02).

References

Allen, J. R. 1981. Beach erosion as a function of variations in the sediment budget, Sandy Hook, New Jersey, U.S.A. *Earth Surface Processes and Landforms* 6 (2):139–50. doi:10.1002/esp.3290060207

Aragonés, L., J. C. Serra, Y. Villacampa, J. M. Saval, and H. Tinoco. 2016a. New methodology for describing the equilibrium beach profile applied to the Valencia's beaches. *Geomorphology* 259:1–11. doi:10.1016/j.geomorph.2015.06.049

Aragonés, L., Y. Villacampa, F. J. Navarro-González, and I. López. 2016b. Numerical modelling of the equilibrium profile in Valencia (Spain). *Ocean Engineering*, 123:164–73. doi:10.1016/j.oceaneng.2016.07.036

Bailard, J. A. 1981. An energetics total load sediment transport model for a plane sloping beach. *Journal of Geophysical Research: Oceans (1978–2012)* 86 (C11):10938–954. doi:10.1029/jc086ic11p10938

Bernabeu, A. M., R. Medina, and C. Vidal. 2003. Wave reflection on natural beaches: An equilibrium beach profile model. *Estuarine, Coastal and Shelf Science* 57 (4):577–85. doi:10.1016/s0272-7714(02)00393-1

Birkemeier, W. A. 1985. Field data on seaward limit of profile change. *Journal of waterway, port, coastal, and ocean engineering* 111 (3):598–02. doi:10.1061/(asce)0733-950x(1985)111:3(598)

Boon, J. D., and M. O. Green. 1988. Caribbean beachface slopes and beach equilibrium profiles. Proceedings of the 21st Conference on Coastal Engineering, Torremolinos, Spain, 1618–30.

Browne, M., B. Castelle, D. Strauss, R. Tomlinson, M. Blumenstein, and C. Lane. 2007. Near-shore swell estimation from a global wind-wave model: Spectral process, linear, and artificial neural network models. *Coastal Engineering* 54 (5):445–60. doi:10.1016/j.coastaleng.2006.11.007

Bruun, P. 1954. *Coast erosion and the development of beach profiles*. Vicksburg: Beach Erosion Board Technical Memorandum. U.S. Army Engineer Waterway.

Crain, D. A., A. B. Bolten, and K. A. Bjorndal. 1995. Effects of beach nourishment on sea turtles: Review and research initiatives. *Restoration Ecology* 3 (2):95–104. doi:10.1111/j.1526-100x.1995.tb00082.x

Da Silva, P. A., A. Temperville, and F. Seabra Santos. 2006. Sand transport under combined current and wave conditions: A semi-unsteady, practical model. *Coastal Engineering* 53 (11):897–13. doi:10.1016/j.coastaleng.2006.06.010

Dean, R. G. 1977. *Equilibrium beach profiles: U.S. Atlantic and gulf coasts. Department of civil engineering. Ocean engineering technical report*. Newark, Delaware: University of Delaware.

Dean, R. G. 1991. Equilibrium beach profiles - Characteristics and applications. *Journal of Coastal Research* 7 (1):53–84.

Dedecker, A. P., P. L. M. Goethals, W. Gabriels, and N. De Pauw. 2004. Optimization of Artificial Neural Network (ANN) model design for prediction of macroinvertebrates in the Zwalm river basin (Flanders, Belgium). *Ecological Modelling* 174 (1–2):161–73. doi:10.1016/j.ecolmodel.2004.01.003

Ecolevante. 2006. Estudio ecocartográfico del litoral de las provincias de Alicante y Valencia, Dirección General de Costas, Ministerio de Medio Ambiente, Spain. Available online: http://www.mapama.gob.es/es/costas/temas/proteccion-costa/ecocartografias/ecocartografia-alicante.aspx.

Foresee, F. D., and M. T. Hagan, 1997. Gauss-newton approximation to Bayesian learning. Proceedings of the International conference on neural networks, Westin Galleria Hotel, Houston, Texas, USA, 1930–35.

Gallant, S. I. 1993. *Neural network learning and expert systems, Massachusetts, USA*, MIT press.

Ghorbani, M. A., R. Khatibi, A. Aytek, O. Makarynskyy, and J. Shiri. 2010. Sea water level forecasting using genetic programming and comparing the performance with artificial neural networks. *Computers & Geosciences* 36 (5):620–27. doi:10.1016/j.cageo.2009.09.014

Govindaraju, R. S. 2000. Artificial neural network in hydrology. II: Hydrologic application, ASCE task committee application of artificial neural networks in hydrology. *Journal of Hydrologic Engineering* 5:124–37.

Grasso, F., H. Michallet, E. Barthélemy, and R. Certain. 2009. Physical modeling of intermediate cross-shore beach morphology: Transients and equilibrium states. *Journal of Geophysical Research: Oceans* 114 (C9).

Hagan, M. T., and M. B. Menhaj. 1994. Training feedforward networks with the Marquardt algorithm. *IEEE Transactions on Neural Networks* 5 (6):989–93. doi:10.1109/72.329697

Hamm, L., M. Capobianco, H. Dette, A. Lechuga, R. Spanhoff, and M. Stive. 2002. A summary of European experience with shore nourishment. *Coastal Engineering* 47 (2):237–64. doi:10.1016/s0378-3839(02)00127-8

Hashemi, M. R., Z. Ghadampour, and S. P. Neill. 2010. Using an artificial neural network to model seasonal changes in beach profiles. *Ocean Engineering* 37 (14–15):1345–56. doi:10.1016/j.oceaneng.2010.07.004

Herman, A., R. Kaiser, and H. D. Niemeyer. 2009. Wind-wave variability in a shallow tidal sea—Spectral modelling combined with neural network methods. *Coastal Engineering* 56 (7):759–72. doi:10.1016/j.coastaleng.2009.02.007

Huang, W., C. Murray, N. Kraus, and J. Rosati. 2003. Development of a regional neural network for coastal water level predictions. *Ocean Engineering* 30 (17):2275–95. doi:10.1016/s0029-8018(03)00083-0

Iglesias, G., I. López, A. Castro, and R. Carballo. 2009. Neural network modelling of planform geometry of headland-bay beaches. *Geomorphology* 103 (4):577–87. doi:10.1016/j.geomorph.2008.08.002

Ihcantabria. 2013. Análisis Matemático y Estadístico de Variables Medioambientales (AMEVA). In ed. U. D. Cantabria. Cantabria, Spain. Available online: http://ihameva.ihcantabria.com/.

Jones, O. P., O. S. Petersen, and H. Kofoed-Hansen. 2007. Modelling of complex coastal environments: Some considerations for best practise. *Coastal Engineering* 54 (10):717–33. doi:10.1016/j.coastaleng.2007.02.004

Kalra, R., M. Deo, R. Kumar, and V. K. Agarwal. 2005. Artificial neural network to translate offshore satellite wave data to coastal locations. *Ocean Engineering* 32 (16):1917–32. doi:10.1016/j.oceaneng.2005.01.007

Karul, C., S. Soyupak, A. F. Çilesiz, N. Akbay, and E. Germen. 2000. Case studies on the use of neural networks in eutrophication modeling. *Ecological Modelling* 134 (2–3):145–52. doi:10.1016/s0304-3800(00)00360-4

Karunanithi, N., W. J. Grenney, D. Whitley, and K. Bovee. 1994. Neural networks for river flow prediction. *Journal of Computing in Civil Engineering* 8 (2):201–20. doi:10.1061/(asce)0887-3801(1994)8:2(201)

Kişi, Ö., and E. Uncuoglu. 2005. Comparison of three back-propagation training algorithms for two case studies. *Indian Journal of Engineering & Materials Sciences* 12 (5):434–42.

Komar, P. D., and M. K. Gaughan. 1972. Airy wave theory and breaker height prediction. Proceedings of the 13th Conference on Coastal Engineering, Vancouver, Canada, 405–18.

Kriebel, D. L., N. C. Kraus, and M. Larson. 1991. Engineering methods for predicting beach profile response. Proceedings of the Coastal Sediments (1991), 557–71.

Larson, M., and N. Kraus. 1995. Prediction of cross-shore sediment transport at different spatial and temporal scales. *Marine Geology* 126 (1):111–27. doi:10.1016/0025-3227(95)00068-a

Lee, T. L. 2008. Back-propagation neural network for the prediction of the short-term storm surge in Taichung harbor, Taiwan. *Engineering Applications of Artificial Intelligence* 21 (1):63–72. doi:10.1016/j.engappai.2007.03.002

Li, G., and J. Shi. 2012. Applications of Bayesian methods in wind energy conversion systems. *Renewable Energy* 43:1–8. doi:10.1016/j.renene.2011.12.006

Mackay, D. J. C. 1992. Bayesian interpolation. *Neural Computation* 4 (3):415–47. doi:10.1162/neco.1992.4.3.415

Masselink, G., and L. Li. 2001. The role of swash infiltration in determining the beachface gradient: A numerical study. *Marine Geology* 176 (1–4):139–56. doi:10.1016/s0025-3227(01)00161-x

Muñoz-Perez, J. J., and R. Medina. 2010. Comparison of long-, medium- and short-term variations of beach profiles with and without submerged geological control. *Coastal Engineering* 57 (3):241–51. doi:10.1016/j.coastaleng.2009.09.011

Muñoz-Perez, J. J., J. M. Gutierrez-Mas, J. M. Parrado, and L. Moreno. 1999. Sediment transport velocity by tracer experiment at Regla beach (Spain). *Journal of Waterway, Port, Coastal, and Ocean Engineering* 125 (6):332–35. doi:10.1061/(asce)0733-950x(1999)125:6(332)

Muñoz-Pérez, J., and R. Medina. 2001. Profile changes due to a fortnightly tidal cycle. 27th International Conference on Coastal Engineering. B. L. Edge. Sydney, Australia, ASCE, 1, 3063–75.

Neill, S. P., A. J. Elliott, and M. R. Hashemi. 2008. A model of inter-annual variability in beach levels. *Continental Shelf Research* 28 (14):1769–81. doi:10.1016/j.csr.2008.04.004

Pan, X., B. Lee, and C. Zhang. 2013. A comparison of neural network backpropagation algorithms for electricity load forecasting. Proceedings of the IEEE International Workshop on Intelligent Energy Systems (IWIES), Vienna, Austria, 22–27.

Pape, L., B. G. Ruessink, M. A. Wiering, and I. L. Turner. 2007. Recurrent neural network modeling of nearshore sandbar behavior. *Neural Networks* 20 (4):509–18. doi:10.1016/j.neunet.2007.04.007

Plant, N., B. Ruessink, and K. Wijnberg. 2001. Morphologic properties derived from a simple cross-shore sediment transport model. *Journal of Geophysical Research* 106 (C1):945–58. doi:10.1029/2000jc900143

Puertos del Estado. 2016. Puertos del Estado. from http://www.puertos.es/en-us/oceanografia/Pages/portus.aspx.

Ranasinghe, R., G. Symonds, K. Black, and R. Holman. 2004. Morphodynamics of intermediate beaches: A video imaging and numerical modelling study. *Coastal Engineering* 51 (7):629–55. doi:10.1016/j.coastaleng.2004.07.018

ROM 0.3-91. 1991. *Recommendation for marine works* 80. Madrid: Ministerio de Obras Públicas y Transportes.

Román-Sierra, J., J. j. Muñoz-perez, and M. Navarro-Pons. 2013. Influence of sieving time on the efficiency and accuracy of grain-size analysis of beach and dune sands. *Sedimentology* 60 (6):1484–97. doi:10.1111/sed.12040

Stive, M. J. F., and H. J. De Vriend. 1995. Modelling shoreface profile evolution. *Marine Geology* 126 (1–4):235–48. doi:10.1016/0025-3227(95)00080-i

Syvitski, J. P. (2007). *Principles, methods and application of particle size analysis* 368. Cambridge, UK: Cambridge University Press.

UNE 103 100. 1995. *Sample preparation for soil tests* 8. Standardization Technical Committee AEN/CTN 103 – Geotechnics.

UNE 103 101. 1995. *Particle size analysis of a soil by screening* 10. Standardization Technical Committee AEN/CTN 103 – Geotechnics.

UNE 7050-2. 1997. *Test sieves. Metal wire cloth, perforated metal plate and electroformed sheet. Nominal size of openings* 8. Standardization Technical Committee AEN/CTN 7 – Materials testing.

Vellinga, P. 1983. *Predictive computational model for beach and dune erosion during storm surges*. Delft Hydraulics Laboratory.

Vellinga, P. 1984. A tentative description of a universal erosion profile for sandy beaches and rock beaches. *Coastal Engineering* 8 (2):177–88. doi:10.1016/0378-3839(84)90012-7

Wang, Q. H. 2004. Improvement on BP algorithm in artificial neural network. *Journal of Qinghai University* 22 (3):82–84. doi:10.3724/sp.j.1010.2010.00136

Yan, B., Q.-H. Zhang, and O. W. H. Wai. 2008. Prediction of sand ripple geometry under waves using an artificial neural network. *Computers & Geosciences* 34 (12):1655–64. doi:10.1016/j.cageo.2008.03.002

Yue, Z., Z. Songzheng, and L. Tianshi. 2011. Bayesian regularization BP Neural Network model for predicting oil-gas drilling cost. Proceedings of the International Conference on Business Management and Electronic Information (BMEI), Guangzhou, China, 483–87.

Table 1. List of profiles on each of the beaches

Beach		Profile	Profile length (m)	Bars	Beach		Profile	Profile length (m)	Bars
1	Almardá	1P – 3P	933.6	No	15	Tabernes de la Valldigna	85P – 94P	1476.3	No
2	Canet de Berenguer	4P – 6P	729.2	No	16	Jaraco	95P – 99P	1111.6	No
3	Alboraya	7P – 11P	758.5	No	17	L'Ahuir	100P – 105P	1099.7	No
4	Cabanyal-Malvarrosa	12P – 16P	707.6	Yes	18	Grao de Gandía	106P – 109P	846.1	No
5	Pinedo	17P – 34P	853.0	Yes	19	Venecia	110P – 111P	661.5	No
6	Saler	35P – 45P	1184.5	Yes	20	Daimuz	112P – 114P	1151.6	No
7	Dehesa	46P – 54P	710.4	Yes	21	Bellreguard	115P – 117P	1153.9	No
8	Recatí	55P – 62P	956.8	No	22	Miramar	118P – 120P	914.3	No

9	Perelló	63P – 65P	803.7	No	23	Piles	121P – 122P	1213.8	No
10	Las Palmeras	66P – 68P	794.9	No	24	Oliva-Terranova	123P – 126P	1195.6	No
11	El Rey	69P – 72P	882.2	No	25	Oliva-Pau Pi	127P – 129P	1076.1	No
12	El Mareny	73P – 75P	801.3	No	26	Oliva-L'Aigua Blanca	130P – 132P	1241.2	No
13	San Lorenzo	76P – 81P	1289.6	No	27	Oliva-Rabdels	133P – 134P	1135.8	No
14	El Dosel	82P – 84P	1628.0	No	28	Oliva-Les Deveses	135P – 140P	919.3	No

Table 2. Correlations between the study variables and the cross-shore profile. Listed in average (ABS) order, where Average (ABS) is the average in absolute value

Variables	y (x = 10)	y (x = 20)	y (x = 40)	y (x = 60)	y (x = 80)	y (x = 100)	y (x = 125)	y (x = 150)	y (x = 175)	y (x = 200)	y (x = 250)	y (x = 300)	y (x = 350)	y (x = 400)	y (x = 450)	Average (ABS)
H_o (PC)	0.284	0.272	0.095	−0.120	−0.231	−0.279	−0.225	−0.066	−0.251	−0.475	−0.266	−0.063	−0.186	−0.283	−0.236	**0.222**
$H_{b,K\&G}$ (PC)	0.288	0.274	0.097	−0.114	−0.224	−0.272	−0.219	−0.061	−0.245	−0.467	−0.252	−0.051	−0.168	−0.280	−0.229	**0.216**
Dir (PC)	−0.336	−0.265	−0.083	−0.019	0.063	0.132	0.135	0.025	0.150	0.328	0.142	0.097	0.200	0.421	0.453	**0.190**
D_{50}	−0.128	−0.102	−0.175	−0.332	−0.352	−0.239	−0.159	−0.114	−0.119	−0.089	−0.119	0.046	0.017	−0.009	−0.008	**0.134**
$H_{b,ROM}$	−0.049	−0.073	−0.061	0.011	0.020	0.071	0.091	0.111	0.110	0.106	0.202	0.208	0.294	0.151	0.204	0.117

(PC)																
Dir (MF)	0.216	0.172	0.099	0.189	0.128	0.116	0.067	0.072	0.066	–0.182	0.082	–0.045	0.073	v0.074	–0.161	0.116
H_o (PC)/L	0.043	0.064	–0.022	–0.193	–0.247	–0.220	–0.158	–0.073	–0.157	–0.239	–0.169	0.003	–0.056	–0.063	–0.023	0.115
H_o (MF)	–0.051	–0.175	–0.162	0.011	0.120	0.071	0.092	0.012	0.111	0.107	0.203	0.139	0.095	0.154	0.207	0.114
Material density (ρ_s)	–0.192	–0.141	–0.032	0.041	0.070	0.073	0.085	0.033	0.081	0.178	0.090	0.097	0.188	0.144	0.214	0.111
H_o (PC)/wT	0,068	0,055	–0,041	–0,175	–0,199	–0,172	–0,131	–0,036	–0,105	–0,198	–0,142	–0,023	–0,071	–0,101	–0,062	0,105
f (PC)	–0.036	–0.019	0.028	–0.024	–0.029	–0.020	0.006	0.009	0.119	0.156	–0.135	**0.168**	**0.213**	**0.282**	**0.330**	0.105

H_o (MF)/wT	0.114	0.074	−0.066	−0.110	−0.111	−0.114	0.0098	−0.0002	−0.056	−0.174	−0.052	−0.025	−0.068	−0.184	−0.153	0.093
f (MF)	0.023	−0.135	−0.021	−0.013	−0.174	−0.017	−0.161	−0.041	−0.050	−0.117	−0.069	−0.126	−0.179	−0.019	−0.234	0.092
Real density (ρ_m)	−0.144	0.028	−0.098	−0.123	−0.054	−0.025	−0.048	0.076	0.053	−0.072	−0.062	−0.099	−0.115	−0.213	−0.177	0.092
$D_{50,DoC}$	0.164	0.154	0.085	0.034	−0.060	−0.152	0.044	−0.035	−0.141	−0.172	−0.030	0.070	−0.016	−0.090	−0.094	0.089
T (ME)	−0.143	−0.067	0.017	−0.012	−0.040	−0.104	−0.138	−0.152	−0.188	−0.120	−0.036	0.147	−0.026	−0.060	−0.063	0.088
T (PC)	−0.028	−0.021	0.015	−0.126	−0.158	−0.143	−0.091	−0.039	−0.101	−0.154	−0.121	−0.026	−0.002	−0.102	−0.174	0.087
H_o (ME)	−0.021	−0.048	−0.052	−0.010	−0.008	−0.053	−0.075	−0.106	−0.090	−0.069	−0.188	−0.135	−0.123	−0.119	−0.172	0.085

H_o (MF)/L	0.059	−0.011	−0.123	−0.195	−0.156	−0.099	−0.088	0.011	−0.008	−0.084	−0.085	−0.021	−0.078	−0.083	−0.128	0.082
Porosity	0.160	0.041	−0.096	−0.129	−0.062	−0.034	−0.057	0.072	0.043	−0.092	−0.073	−0.011	−0.135	−0.027	−0.199	0.082
T (MF)	−0.019	0.029	0.018	−0.128	−0.162	−0.149	−0.096	−0.040	−0.107	−0.066	−0.027	0.024	−0.004	−0.092	0.163	0.075
H_o (ME)/wT	0.019	0.004	−0.057	−0.142	−0.155	−0.148	−0.096	−0.052	−0.090	−0.153	−0.076	0.037	−0.018	−0.009	0.034	0.073
Dic (ME)	−0.090	−0.079	−0.196	−0.094	−0.054	−0.046	−0.028	−0.021	0.025	0.017	0.158	0.076	0.078	−0.058	−0.053	0.072
f (ME)	0.230	0.136	0.009	−0.033	−0.082	−0.032	0.006	0.075	0.112	0.081	0.108	−0.068	−0.010	0.025	−0.027	0.069
H_o (ME)/LL	−0.010	−0.029	−0.020	0.011	0.007	−0.062	−0.030	−0.058	−0.073	−0.062	0.046	0.119	0.035	0.001	0.017	0.039

Figure 1. Location of the study area and morphology of the seabed.

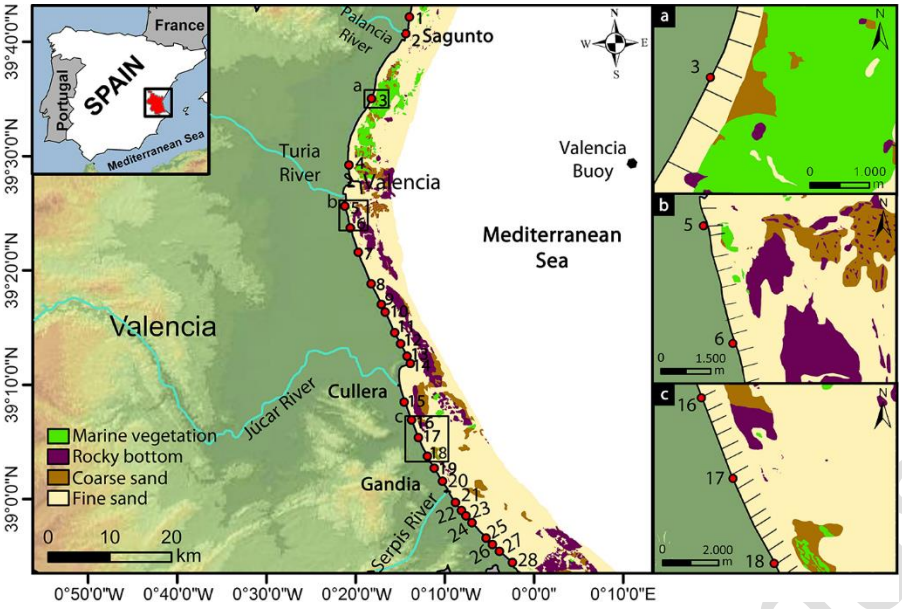

Figure 2. Average of R^2 values and the standard deviation for each of the 20 neurons for each model.

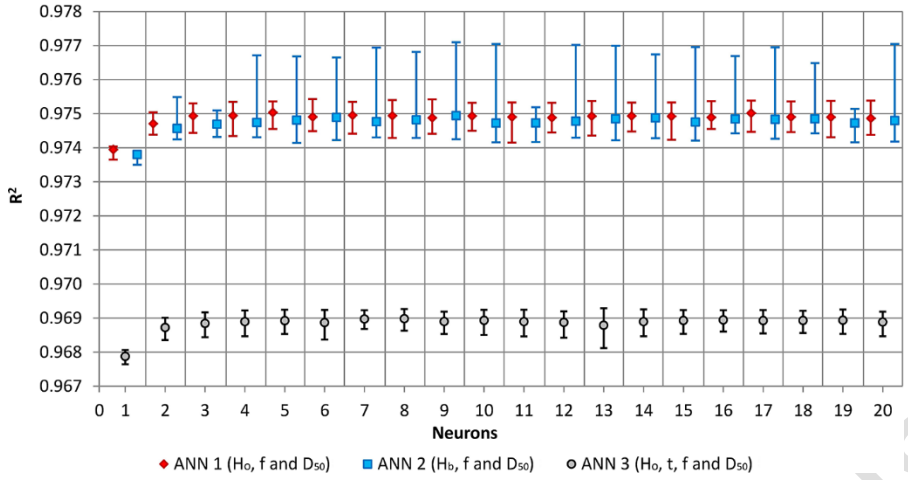

Figure 3. Absolute error (m) of the ANN 1 [3–3–15] and the model of Aragonés in each profile.

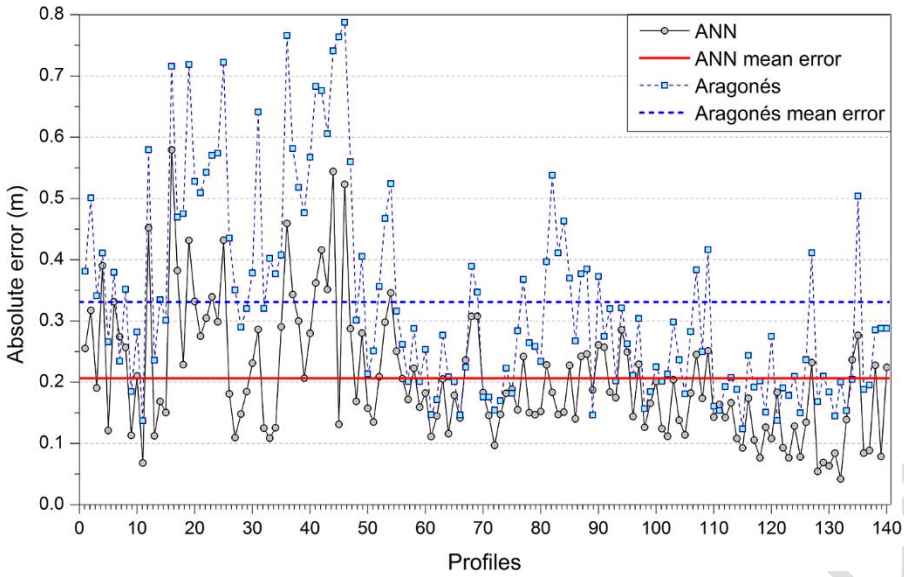

Figure 4. Absolute error (m) of the ANN 1 [3–3–15] and the model of Aragonés in each beach.

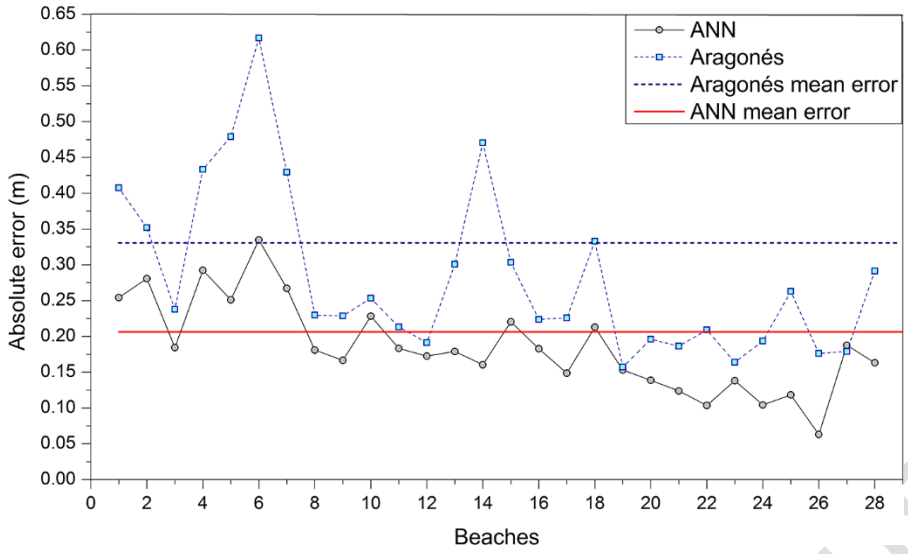

Figure 5. MAPE and δ of the ANN 1 [3–3–15] and Aragonés model at each beach.

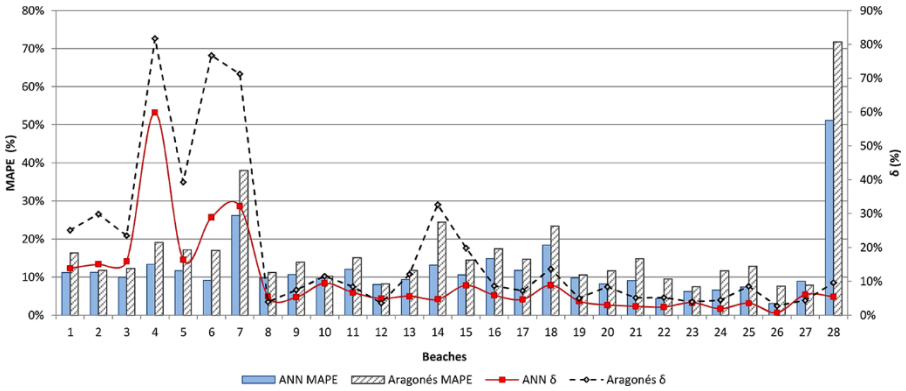

Figure 6. between measured profiles and the profiles obtained from the ANN 1 [3–3–15] and the model of Aragonés in the bar area.